We are IntechOpen,
the world's leading publisher of
Open Access books
Built by scientists, for scientists

4,800

Open access books available

122,000

International authors and editors

135M

Downloads

Our authors are among the

154

Countries delivered to

TOP 1%

most cited scientists

12.2%

Contributors from top 500 universities

BOOK CITATION INDEX
CLARIVATE ANALYTICS
INDEXED

WEB OF SCIENCE™

Selection of our books indexed in the Book Citation Index
in Web of Science™ Core Collection (BKCI)

Interested in publishing with us?
Contact book.department@intechopen.com

Numbers displayed above are based on latest data collected.
For more information visit www.intechopen.com

Digital Image Processing for Quality Control on Injection Molding Products

Marco Sasso, Massimo Natalini and Dario Amodio
Università Politecnica delle Marche
Italy

1. Introduction

The need to increase quality of products, forces manufacturers to increase the level of control on finished and semi-finished parts, both qualitatively and quantitatively.

The adoption of optical systems based on digital image processing is an effective instrument, not only for increasing repeatability and reliability of controls, but also for obtaining a large number of information that help the easily management of production processes.

Furthermore, the use of this technology may reduce considerably the total amount of time needed for quality control, increasing at the same time the number of inspected components; when image acquisition and post-processing are feasible in real time, the whole production can be controlled.

In this chapter we describe some quality control experiences carried out by means of a cheap but versatile optical system, designed and realized for non contact inspection of injection moulded parts.

First, system architecture (both hardware and software) will be showed, describing components characteristics and software procedures that will be used in all the following applications, such as calibration, image alignment and parameter setting.

Then, some case studies of dimensional control will be presented. The aim of this application is to identify and measure the main dimensional features of the components, such as overall size, edges length, hole diameters, and so on. Of particular interests, is the use of digital images for evaluation of complex shapes and dimension, where the distances to be measured are function of a combination of several geometric entities, making the use of standard instrument (as callipers) not possible. At the same time, methods used for image processing will be presented. Moreover, a description of system performances, related to quality product requirements will be presented.

Second application examines the possibility to identify and quantify the entity of burrs. The case of a cylindrical batcher for soap, in witch its effective cross-sectional area have to be measured will be showed, together with a case study in witch burrs presence could bring to incorrect assembly or functionality of the component. Threshold and image subtraction techniques, used in this application will be illustrated together with the big number of information useful to manage production process.

Third, it will be presented a possible solution to the problem of identifying general shape defects caused by lacks of filling or anomalous shrinkage. Two different approaches will be

used, the former that quantifies the general matching of whole images and the latter that inspects smaller areas of interest.

Finally, an example of colour intensity determination of plastic parts for aesthetic goods will be presented. This application has the aim to solve the problem of pieces which could appear too dark or too light with respect to a reference one, and also to identify defects like undesired striation or black point in the pieces, depending on mixing condition of virgin polymer and masterbatch pigment. Use of pixel intensity and histograms have been adopted in the development of these procedures.

2. System description

In this section, the hardware and software architecture of the system will be described.

The hardware is composed by a camera, a telecentric zoom lens, two lights, a support for manual handling of pieces, and a PC.

The camera is a monochromatic camera with a CCD sensor (model AVT Stingray F201B ®). The sensor size is 1/1.8", and its resolution is 1624 x 1234 pixel, with a pixel dimension of 4,4 µm, a colour depth of 8 bit (256 grey levels) and a maximum frame rate of 14 fps at full resolution. The choice of a CCD sensor increases image quality, reducing noise in the acquisition phase and the high resolution (about 2 MPixel) leads to an acceptable spatial resolution in all the fields of view here adopted.

The optics of the system is constituted by a telecentric zoom lens (model Navitar 12X telecentric zoom.®); the adopted lens is telecentric because it permits to eliminate the perspective error, which is a very useful property if one desires to carry out accurate measurements. The zoom system permits to have different field of view (FOV), so the FOV can vary from a minimum of 4,1 mm to a maximum of 49,7 mm. The zoom is moved by a stepper driving, and the software can communicate and move it automatically to the desired position. The utility of this function will be clear later, when the start-up procedure is explained.

The depth of focus varies with the FOV, ranging from 1,3 mm to 38,8 mm; the mentioned camera and lens features bring to a maximum resolution of the system of 0,006 mm (FOV 4,1 mm) and a minimum resolution of 0,033 mm (FOV 49,7 mm).

To lights the scene, a back light and a front light were adopted. Both have red light, to minimize external noise and to reduce chromatic aberration. Moreover they have a coaxial illumination, that illumines surface perpendicularly and increases contrast in the image highlighting edge and shapes and improving the general quality of the image. In figure 1.a the complete system is showed. All the components are managed by a PC, that use a specific software developed in LabView®.

Its architecture is reported in figure 1.b. It has a user interface, that guides step by step the operator through the procedures for the different controls. So, the operator is called only to choose the application to use, then to load pieces in the work area and to shot photos. Every time he shots, image is acquired and processed (and stored if necessary), so the result is given almost immediately. If the operator needs to control a production batch, it is also possible to acquire several images consecutively and then post-process all of them exporting global results in an excel file.

All this operations are possible thank to the background software, that answer to the operator input. In fact, when the operator select the kind of control, the software load all the parameters necessary to the analysis. For each application, the software load all parameters

for camera, zoom and lights (that have been stored earlier), and all the information about the analysis, like calibration, templates for image alignment and so on.
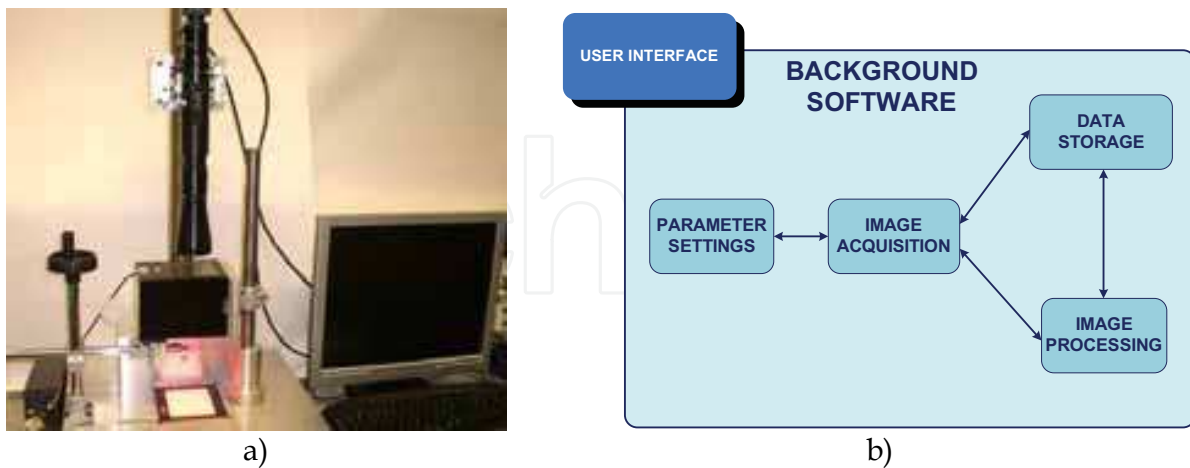

Fig. 1. a) Hardware architecture; b) Software architecture

With regard to camera settings, the software controls all parameters like time exposure, brightness, contrast and so on, so when the best mix of parameters had been determined for a given application, for the analysis is enough to call it back. The same happens for the zoom control; in fact the software loads the position stored for the selected application and commands to the zoom driver to move in that position. This is useful because, if necessary, the system can acquire images of a large FOV to get information about certain features, and then narrows the FOV and acquire images with higher spatial resolution for capturing smaller details in the observed object. Each position utilised has been calibrated sooner. When a position is called, the software restores related parameters, and pass them to the following step for elaboration. The software also control light intensity, in the same way of previous components. So, all the information are passed to the acquisition step and then stored in the acquired images.

After this overview of the system, it's proper to describe two functions that are used in all applications before any other operation: image calibration and image alignment.

2.1 Image calibration

Using digital images, two kind of calibration are necessary: spatial calibration (always) and illumination and acquisition parameters calibration (depending on material and shape of the pieces to be analysed).

Spatial calibration convert pixel dimensions into real world quantities and is important when accurate measurements are required. For the application described below, a perspective calibration method was used for spatial calibration (NI Vision concept manual, 2005). So, the calibration software requires a grid of dots with known positions in image and in real world. The software uses the image of the grid and the distance between points in real world to generate a mapping function that "translates" the pixel coordinates of dots into the coordinates of a real reference frame; then the mapping can be extended to the entire image. Using this method is possible to correct perpendicularity error of camera and scene which is showed in figure 2a. This effect is actually rather reduced in the present system, as the support has been conceived to provide good mechanical alignment by means of a stiff column, that sustains camera in perpendicular position with respect to the scene.

This method of calibration is however useful and must be used to correct also alignment error (or rotation error) between image axis and real world axis (fig. 2b). It is also possible to define a new reference system in the best point/pixel for the studied application (for example, at the intersection of two edge of the piece analysed).
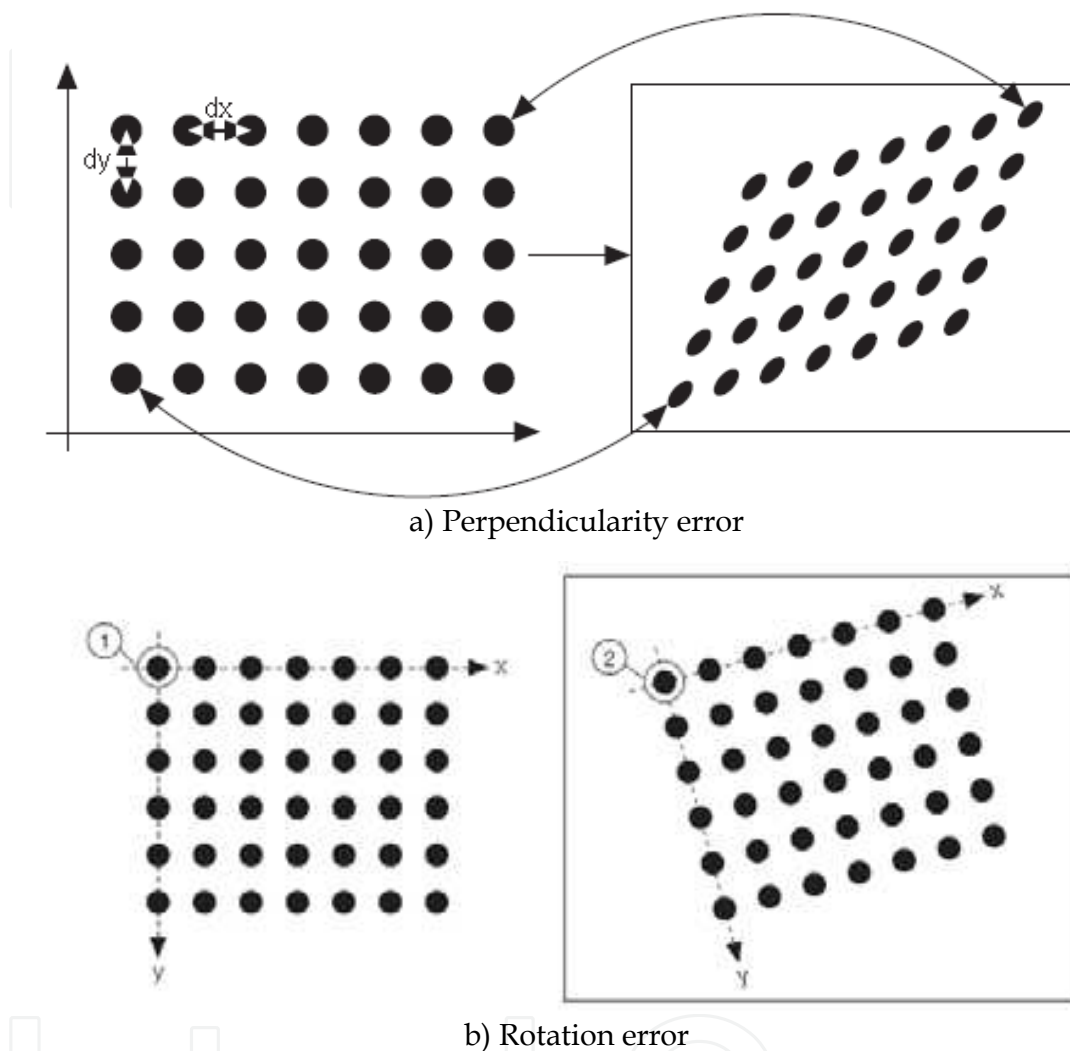
a) Perpendicularity error

b) Rotation error

Fig. 2. Errors to correct in image calibration

About parameter setting, the problem is represented by transient materials because the light passes through the material and the dimension measured changes with intensity of illumination. So a simple method was used to correct this effect. A master of the pieces to analyse was manually measured with calliper, and the acquisition parameters (particularly brightness, contrast ant time exposure of the camera) were selected to obtain the same results with digital image measurement. All this parameters are stored for each application.

2.2 Image alignment
The other operation computed by the software before each analysis is the image alignment. This operation simplifies a lot the pieces positioning and make the analysis much easier and faster for the operator. In fact the pieces have to be positioned manually in the FOV so it is very difficult to put them always in the same position to permit the software to find features

for measurement. In order to align every image with the master image that was used to develop the specific analysis tool, it could be even possible to put a given piece in any position within the field of view, and let then the software to rotate and translate the image to match the reference or master image thus to detect features and dimensions. However, for the sake of accuracy and repeatability, the positioning is aided by centring pin and support that permit to place the objects in positions that are similar to the master one used for calibration and parameters setting.

The alignment procedure is based on pattern (or template) matching and uses a cross-correlation algorithm. So, first is necessary to define a template (fig. 4b) that the software consider as a feature to find in the image. From this template, the software extracts pixels that characterize the template shape, then it looks for the pixel extracted in the new image, using an algorithm of cross-correlation; so is possible to consider the template as a sub image $T(x,y)$ of size K x L in a bigger image $f(x,y)$ of size M x N (see fig. 4), and the correlation between T and f at the pixel (i,j) is given by (J. C. Russ, 1994):

$$C(i,j) = \frac{\sum_x \sum_y T(x,y) \cdot f(x+i,y+j)}{\sqrt{\sum_x \sum_y f^2(x+i,y+j) \cdot \sum_x \sum_y T^2(x,y)}} \tag{1}$$

Correlation procedure is illustrated by fig.3. Correlation is the process of moving the template $T(x,y)$ around the image area and computing the value C in that area. This involves multiply each pixel of the template by the image pixel that it overlaps and then summing the results over all the pixels of the template. The maximum value of C indicates the position where T best matches f.
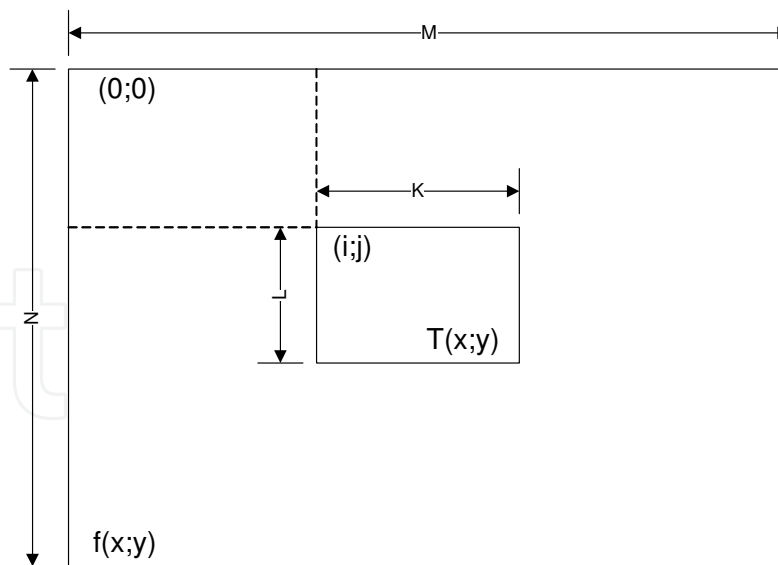

Fig. 3. Correlation process

This method requires a big number of multiplications, but is possible to implement a faster procedure: first, the correlation is computed only on some pixels extracted from the template, to determines a rough position of the template; then, the correlation over all pixels of the template can be executed in a limited area of the entire image, allowing to reduce processing time.

In fig. 4 the method applied to the first case of study is showed. Fig. 4.a reports the master image, from which the template (fig. 4b) has been extracted. It's clear, that only a part of the master image has been extracted and this part is considered as the feature to be searched in the entire image. In fig. 4.c is showed an image of a piece to align with the master, in fact, in this image, the piece has been moved behind and rotated. The software, first search the template and determines his rotation angle, rotates the image of the same entity to align the new image to the master. Then it finds the new position of the template and determines the translation vector from the master, moves the image of the fixed quantity and the new image is now aligned to the master. Black areas in fig. 4.d, are the results of translation and rotation of image; they are black because these areas have been added by the process, and a part of the image has been deleted to keep the same size of the original image. A double pattern matching is necessary, because of the image reference system is located on the left top of the image and not in the template centre. So, first pattern matching determines the rotation angle and the translation vector that have to be applied but uses only the first to rotate the image. Performing this operation in fact, the new image has the same alignment of the master image, but the translation vector changes because the rotation is performed respect to the left up corner of the image. Second pattern matching determines yet the angle (that now is zero) and the new translation vector that is used to move the image to the same position of the master. Image can be now processed.
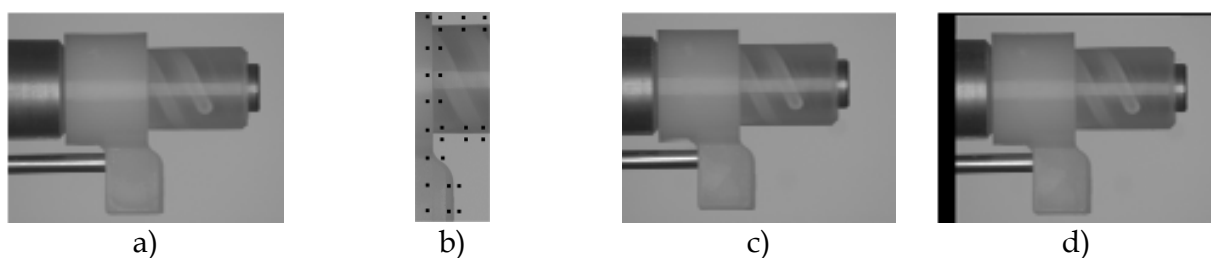

Fig. 4. The alignment process applied to the first case of study

3. Dimensional measurement

This section describes some examples of dimensional measurement on injection moulded parts.
In fig.5.a it is shown a 3D simplified model of the part to analyse. It is constituted by two coaxial cylinders, with a ribbing on the left side; the material is Polyamide 66 (Zytel 101). In fig. 5.b, all the features that have to be measured in quality control process are represented. It's important to notice that there are two kind of feature to measure. The dimensions denoted by numbers 1, 3 and 4 require the identification of two simple feature (edges) of the part, so this will be a "simple feature" to measure, and a comparison with standard instrument is possible. Instead, feature number 2, requires the identification of an axis, by identification of two edges, and the identification of third element (edge of the ribbing) to measure the distance from the latter to the previous axis. So, three features are required and is impossible to get this measurement with standard instruments like gauges or callipers. This represent a second kind of measurement, that will be called "composed feature".
Both cases pass through the identification of edges, so the procedure used for their detection will be now described.

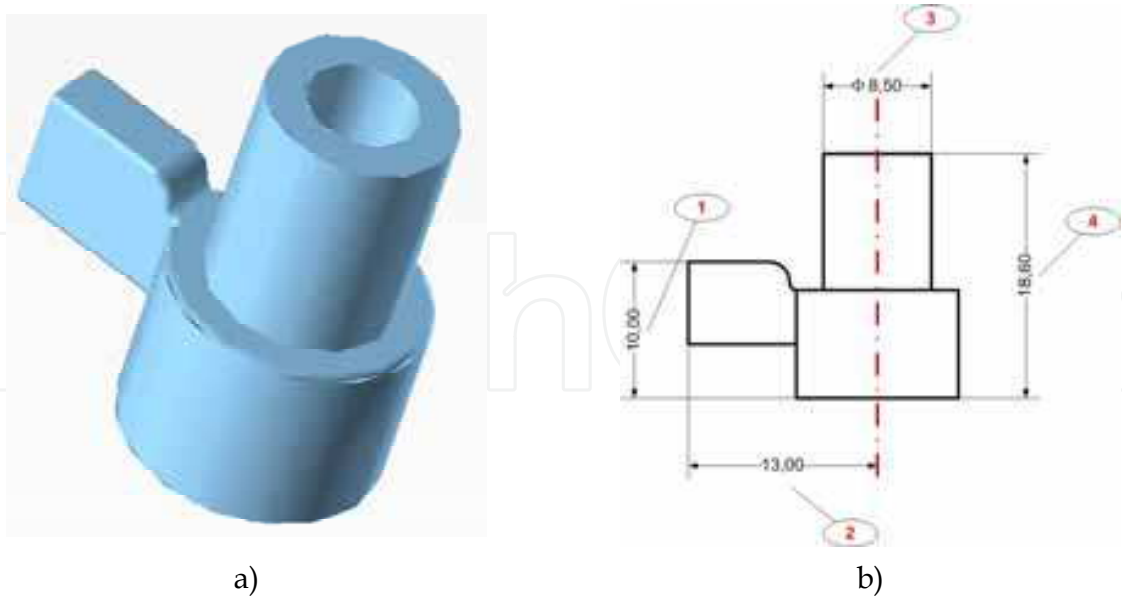a)   b)

Fig. 5. a) the piece to analyse, b) requested features

More techniques are based on use of pixel mask that runs through the image, computing the sum of products of coefficients of pixel mask with the gray level contained in the region encompassed by the mask. The response of the mask at any point of the image is (Gonzales & Woods, 1992):

$$R = w_1z_1 + w_2z_2 + ... + w_9z_9 = \sum_{i=1}^{9} w_i z_i \qquad (2)$$

where: w_i = coefficient of the pixel mask;
         z_i = gray intensity level of the pixel overlapped.

Using different kind of mask, different features can be detected. All of them, are detected when:

$$|R| > T \qquad (3)$$

where T is a nonnegative threshold. Fig. 6 shows different masks for detection of different features.

-1	-1	-1
-1	8	-1
-1	-1	-1

-1	-1	-1
2	2	2
-1	-1	-1

-1	2	-1
-1	2	-1
-1	2	-1

-1	-1	2
-1	2	-1
2	-1	-1

2	-1	-1
-1	2	-1
-1	-1	2

a)Point   b)Horizontal edge   c)Vertical edge   d)+45° edge   e)-45° edge

Fig. 6. Different pixel mask for different features

In this application, an easier method, based on pixel value analysis along a pixel line, has been used. It is a simplification of derivative operators method (Gonzales & Woods, 1992) that uses gradient operators and analyses gradient vector to determine module and direction of the vector.

Usually, an edge is defined as a quick change in pixel intensity values, that represents boundaries of an object in the FOV. It can be defined by four parameters:

1. Edge strength: defines the minimum difference in the greyscale values between the edge and the background;
2. Edge length: defines the maximum distance in which the edge strength has to be verified;
3. Edge polarity: defines if the greyscale intensity across the edge is rising (increase) or falling (decrease);
4. Edge position: define x and y location of an edge in the image.

In picture 7.a is represented a part of an edge (black rectangle); first, the software requires the input of a user-defined rectangle (green in fig 7.a) that it fixes as the ROI in which to look for the edge. Then the software divides the rectangle using lines parallel to a rectangle edge, in the number specified by the user (red arrows in fig. 7.a), and analyses greyscale value of each pixel line defined, moving from the start to the end of the arrow if a rising edge is expected, vice versa if a falling edge is expected. Now It defines a steepness parameter, that represents the region (the number of pixels) in which the edge strength is expected to verify. Then, the software averages the pixel value of determinate number (width of filter) of pixel before and after the point considered. The edge strength is computed as the difference between averaged value before and after edge steepness. When it finds an edge strength higher than expected edge strength, it stores the point and continues with the analysis until the maximum edge strength is reached. Now, the point found in this way is tagged as edge start and the steepness value is added to find the edge finish. Starting from edge finish, the first point where the greyscale value exceeds 90% of starting greyscale value is set as edge position. Figure 7.b show the determination process of the edge and fig. 7.a shows the edge position determinate (yellow points).

ROI used for edge detection   Edge position determination

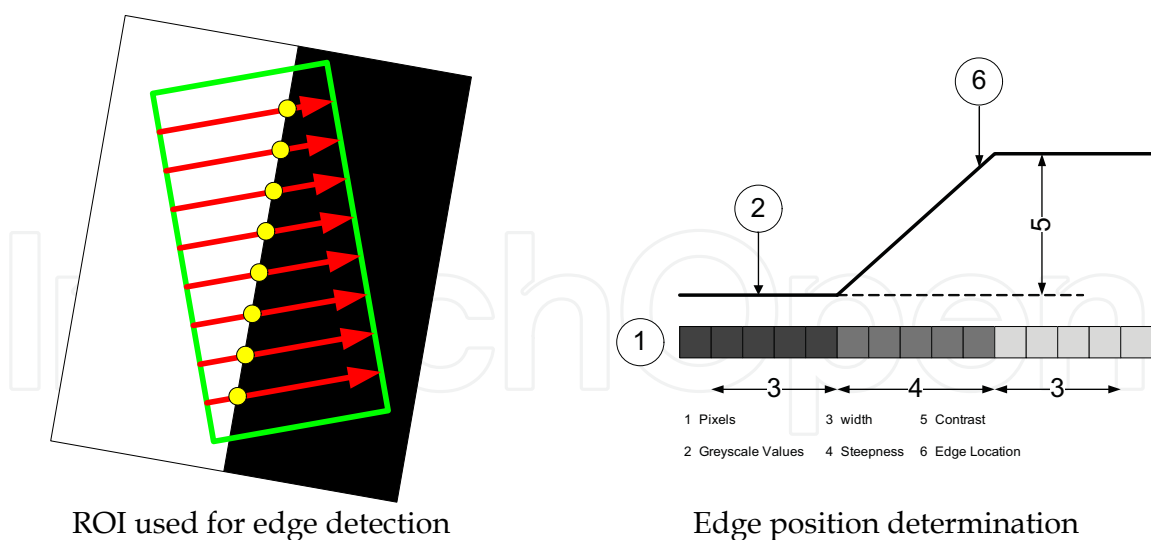Fig. 7. Determination process of edge position

It's clear that parameter settings influence edge position, especially when translucent material are analysed. In fact, translucent materials are characterised by lower greyscale intensity changes and high steepness values. If external noise cannot be eliminated appropriately, it could be difficult to get high repeatability in edge positioning in the image.

This can be avoided applying filters to the image before edge determination process. In this application, a filter to increment contrast was applied. This allow to reduce the steepness to two pixels only, and the filter width also to four pixels only. In fig.8 filter effects on the image are shown; fig. 8.a represents the original image acquired, fig. 8.b reports filtered image with increased contrast.

a)   b)
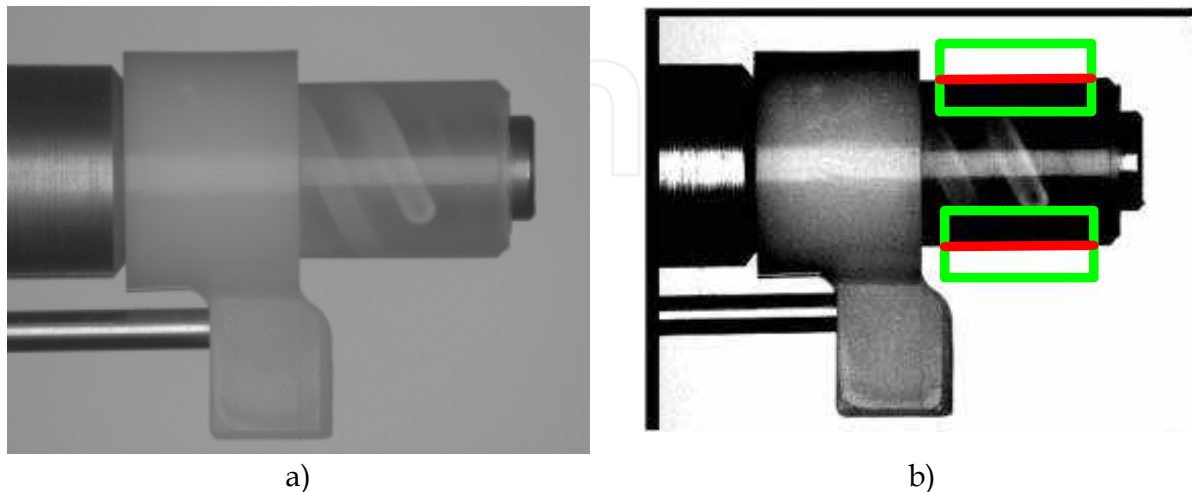
Fig. 8. a) original image, b) aligned and filtered image

To increment contrast in the image, it's also possible to increment illumination intensity but in this case the light passes through the material in a huge way and the dimension of the part will be undervalued, so this method have to be used carefully.

This process have to be done confronting image results with contact methods or other suitable techniques; in particular, standard caliper measurement was used here.

3.1 Simple feature measurement

In this section, measurement process of simple feature will be illustrated. A simple feature is a feature that requires the identification of two elements, then some dimensional or geometric information are extracted by them. Features number 1, 3 and 4 of fig. 6.b are representative of this case. Feature number 1 will be treated as example. The objective is to determine the diameter of the part. As previously explained, two search areas have to be determined. The region may have the desired shape (circular, rectangular, square, polygonal) depending on the feature to inspect. In this case, because a line is searched, two rectangular ROI are defined (green rectangles in fig. 8.b). The ROI has fixed size and fixed position in the image; hence, alignment process is important in order to bring the part always in the same position in the image, permitting the software to find the edge at all times, with high reliability and robustness. A rake division of five pixels has been used (distance between each inspection line), it means that a point every 0,085 mm is stored (about 40 points per line). When points are determined, they are used to fit a line with a linear regression method and to determine the equation of the line in the image.

Once the equation has been determined, the process is repeated for the second edge, to determine the second equation. The rectangular search area is the same and has the same x position; this is important to define distance in following steps.

Now, using the equations is possible to find all the information required analytically. Defining first line as reference line, maximum and minimum distance between the lines has

been computed (the distance between extreme points) and has been averaged, to find medium distance between edge; also parallelism error can be evaluated as the difference between maximum and minimum edge distances. For each piece, two information have been obtained: medium distance and geometric error.

The edge determination is applicable also to other feature, such as holes; indeed, in the following case study the problem of a threaded hole is treated, where the inner diameter has to be measured.

a)   b)   c)
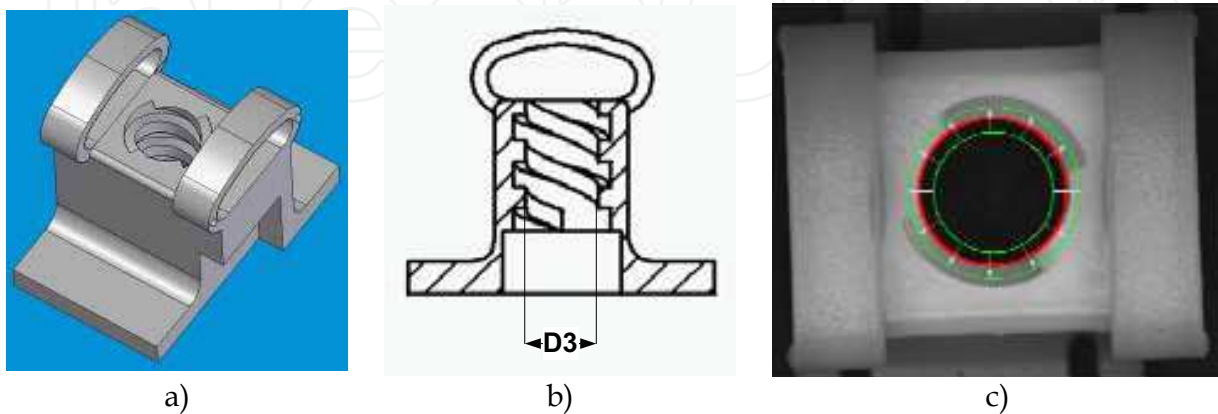
Fig. 9. A problem of inner diameter determination

Traditional methods used for control process employs go-no-go gauges for diameter verification. So it is possible to say that inner diameter is comprised between established tolerance range (minimum and maximum dimension of gauges) but it's impossible to get an exact value of the diameter. The use of a standard gauge is difficult because there are not plane surfaces. Digital images offers a good solution. It is possible to determine a circular edge with the same method explained before, having care of changing the search area which now has to be annular (green circles in fig. 9.c), with inspection lines defined by their angular pitch along the circumference (white arrows in fig. 9.c). The result is the red circle reported again in fig. 9.c, which is the circle that best fits the detected circumference points.

3.2 Composed feature measurement

In this section, the measurement of feature 2 (fig. 5.b) will be explained briefly, as it can be carried out by a simple extension of the procedures already developed.

Now, the aim is to determine the distance between the ribbing edge and the axis of the hollow cylinder identified before and whose diameter has been measured. So the feature involved are three. The procedure can be similar to the previous: starting from the cylinder edges already determined (see fig.8.b), the equation of their medium axis can be easily calculated (the axis is reported in fig.10.a). Also the ribbing edge is determined with the procedure illustrated before (red in fig. 10.a), and the distance between the axis and the rib edge can be evaluated easily and quickly by analytical computations.

The same method can be applied in all that situation when it's necessary to locate any feature in the image. For example, locate the position of an hole respect to the reference system or a reference point, given by intersection of two edges; figure 10.b shows the process. The measurement can be composed as many time as desired, including all the feature that can be identified in the FOV.
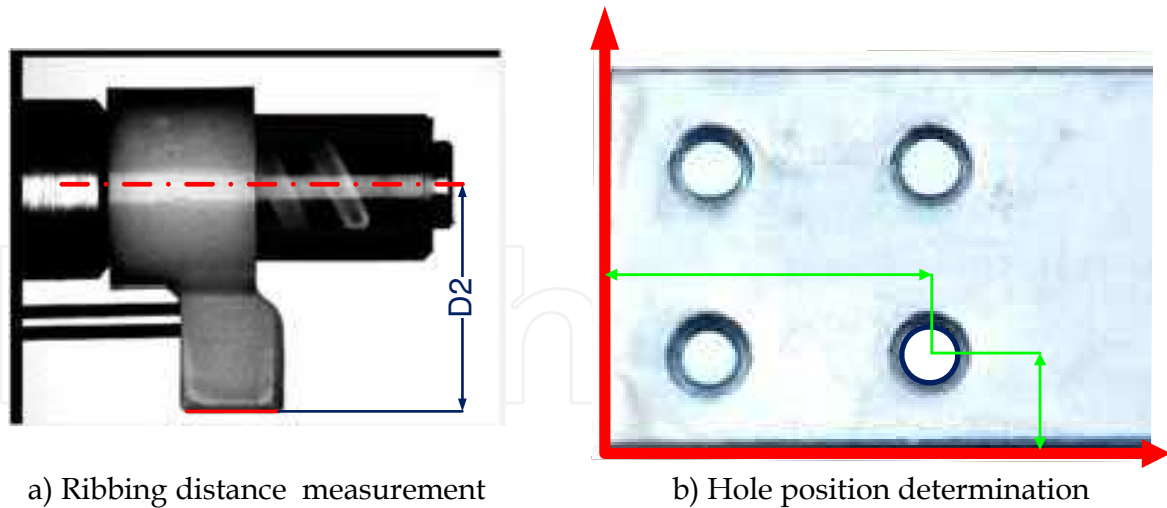
a) Ribbing distance measurement   b) Hole position determination

Fig. 10. Process of composed feature measurement

4. Area measurements

Digital images are suitable also to measure 2D features, such as areas. In this section two cases of study will be illustrated. In the first example, the problem is represented by a burr caused by non perfect adherence between mould parts; the aim is to identify and measure the entity of the burr (fig. 11.a). The second problem is again about burr occurrence on the edge, as marked with a blue line in fig. 11.b, but the aim is to measure the area free from burr, available for fluid flow. The pictures also report the real image of burrs in the parts. In the first case burr covers only a part of the edge, while in the second example it extends all along the edge circumference.

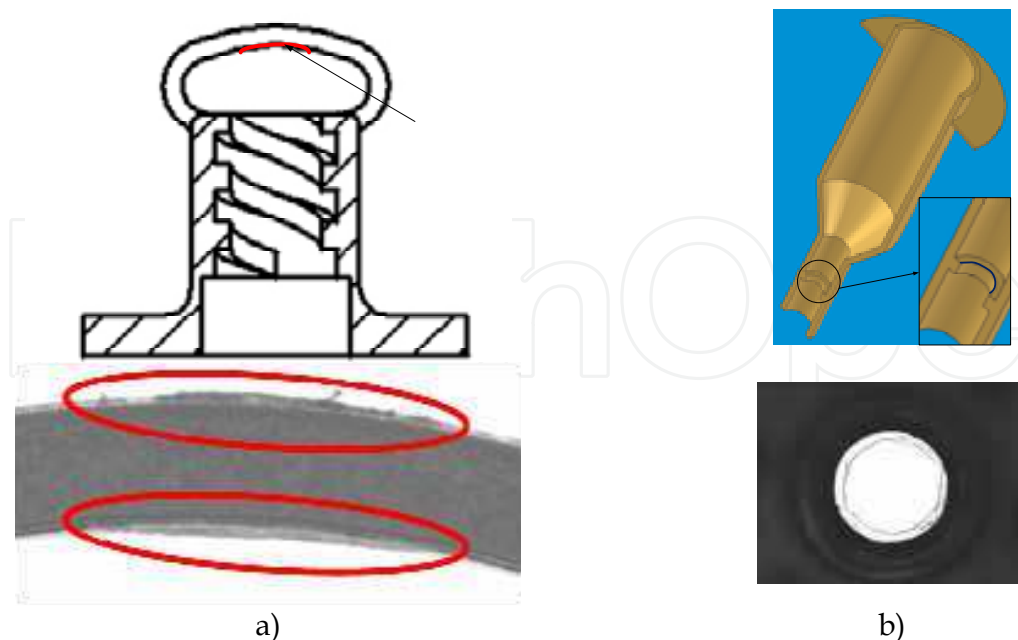a)   b)

Fig. 11. Burrs identification and quantification on two different parts

To quantify the entity of the burrs, instruments like contour projector are used. The only information available from the analysis is the maximum height of burr and it is inadequate

to determine precisely the free area of the hole, or the extension on the edge. Digital images solve the problem using a combination of threshold and binary operation, so these two techniques will be now explained.

In a few words, in the digital images here presented, parts are characterised by an intensity range of gray-level much different from the background. Pixels of the part have a gray-level intensity comprised in a given interval, while all other pixels not included in this intensity range can be considered as background. Threshold operation sets all pixel that belong to the desired interval to a user-defined value, typically 1, and all other pixel of the image to zero. The image obtained is a binary image.

First case presents a burr, that has a gray-level between the free-area (gray-level ≥ 250) and the part (gray-level ≤ 120). The software, after alignment operation, extracts the zone of the image interested by analysis (fig 12.b); then, it performs a first binarization on this sub-image with a threshold value of 250, settings to 255 all pixels with a gray-level lower than 250 in order to obtain the area of the part and the burr together (fig. 12.c). To the same image extracted, a new binarization is applied, with a gray-level value of 138, and all pixel with a lower gray-level value are set to 255 to obtain the area of the part only (fig. 12.d). Finally, image in fig. 12.d is subtracted by fig 12.c to separate the burr areas. Now, with procedures similar to those used in edge detection, it is possible to determine search areas in which ROI lines are defined to identify edges. In this application an edge every 5 pixel has been determined and measured, and the software extracts the maximum value within them and returns it as measurement result. In this way, only and always the maximum burrs height is considered in measurement results. This method is conservative, but gives the certainty that the defects entity will not exceed the part requirement limits.

a)   b)   c)   d)   e)
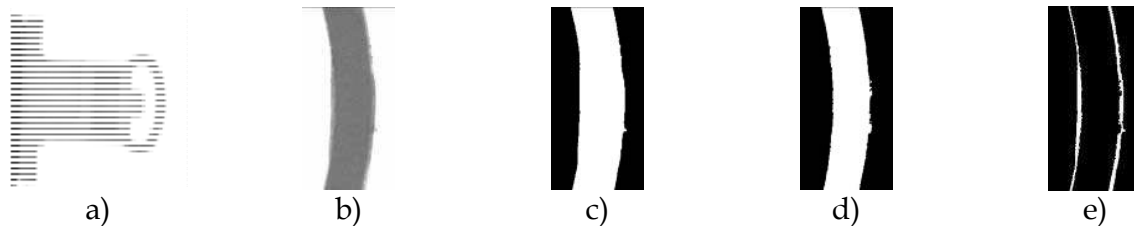
Fig. 12. Burr determination process

It's important to underline that is possible to obtain other information on burrs, that cannot be extracted with traditional methods. For example, one can measure the area (this procedure will be explained later) to understand the entity of the problem; a thin burr along all the edge indicates a defect solvable by proper tuning of injection process parameters, while big area localized on a small part of the edge indicates a damage on the mould. Furthermore, it is also possible to determine x and y mass centre position to understand where the mould is damaged. So, much more parameters are available to control production process and it is easier to define a set of them that indicates the need to repair the mould.

In the case of fig. 11.b, a different procedure that uses threshold method has been applied. Now the problem is to measure correctly the free area for fluid flow. With standard methods is only possible to have an approximation, measuring the burr height and computing the area of the annular region occupied by burr. But if this area is not annular or presents an irregular form, then it is almost impossible to get a precise measurement of its extension.

Using digital images, it is possible to implement a series of operations that compute the area with a good precision and automatically.

Since the free area has the highest gray-level of the image, the software developed computes the mass centre of the image (substituting mass with pixel gray-level values, obviously) which will always fall in the free area. From this point, the software begins to select all the pixels having a gray-level comprised in a properly defined range. Since a free area is looked for, a value of 255 has been set, with a tolerance of 5 gray-level. The algorithm stops at the burr edge, when it find a gray-level lower than 250. At the end of selection process, the software counts the number of pixel selected and, applying calibration information determines the area available for fluid flow. In fig. 12.a is reported the image before processing, and fig. 13.b shows the processed image.

a)   b)

Fig. 13. The process of free area extraction

A brief explanation about threshold level must be given: smaller is the tolerance range, smaller will be the area extracted; using a tolerance range of zero, only the pixels with a gray-level of 255 will be selected and the resulting area will be the smaller as possible. In this application, the fluctuation is negligible, but this must be verified for each case and the most appropriate range has to be selected.

5. Shape defects

Digital images can also be used not only in measurement applications, but also for all controls that involve aesthetic and functionality aspects of moulded parts. This kind of controls is generally executed by expert operators, that have a depth knowledge of the process and of the part. A big experience is required and a proper training for operators is necessary. In spite of all, the work of qualified operators is not always enough for getting high product quality, because often fixed tolerance ranges are not given, and the entity of defects can be judged differently from different operators. Moreover, this kind of defects are frequently not measurable with standard instruments, and it is not easy to define a parameter to measure, check and certify part quality.
In this section, some examples of shape defects detection by digital images will be showed.
First will be explained the case of a thread termination damage.
The part of fig. 9.a has a thread in his centre, realized by a core that in his terminal part contacts the fixed plate of the mould (interested zones are highlighted by red lines in fig. 14.a). These parts of the core are very thin, and because of their low resistance property, they are the parts of the mould to undergo damage in production process earlier. If this part of the core is broken, the injection moulded component will have a defected shape that not allows the coupled screw to slide in him.
Fig. 14.b shows a correct thread termination, while fig. 14.c shows a damaged thread termination. The difference is quite small and difficult to see for a human eye that is performing many checks repeatedly. Nevertheless, carrying out a quantitative measure of

such damage is basically impossible with standard instruments. Instead, using digital images it is possible to establish a procedure to determine a quantitative measure of the defect, that is a number which should be compared with admissible tolerance limits.
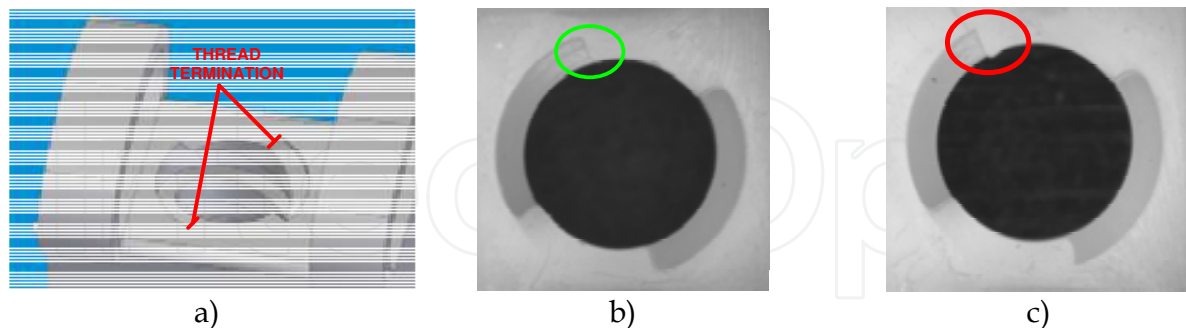

Fig. 14. a) the particular; b) Good thread termination; c) Damaged thread termination

First step is always constituted by image alignment. In this case the part is aligned with image reference system, using external edges of the part, then the inner diameter of the thread is determined together with his centre (fig. 15.a); the thread termination edge is determined (green in fig. 15.b, indicated by green arrow) and the horizontal distance (indicated by P) between edge centre and thread centre is determined (fig. 15.c). This parameter has been selected because of its great sensitivity with respect to even small damages of the thread. Now is also possible to set a tolerance range within which the part can be accepted.
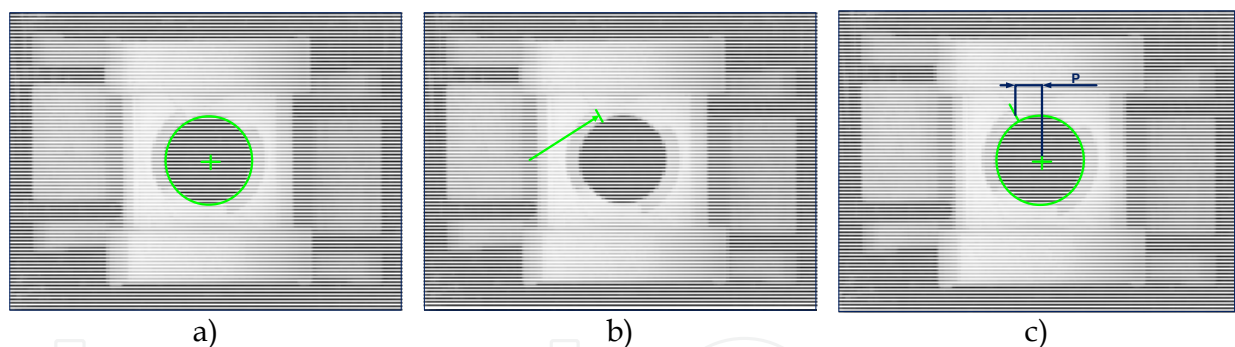

Fig. 15. Measurement process of damaged thread

Here, the maximum distance accepted is 1 mm, which has been chosen analyzing more than 100 good pieces, and assuming the greater dimension as the maximum tolerance limit. Over this limit, the software alerts the operator with a warning message suggesting to reject the part.   It's proper to note that expert operators are not required, because now the measurement process is totally automated and the interpretation is not subjective; however, this theme will be discussed more deeply in next section.

Next case presented below, is about individuation of process defects. To do this, part in fig 8.a will be considered. In moulding process, this particular often presents problems as short shot (fig 16.a, absence of ribbing) and air bubbles on the ribbing and on the cylinder (fig 16.b and 16.c respectively).

Different inspection methods are used, depending on what is the defect looked for. In fact, for short shot defect that is generally easy to detect, a simple pattern matching could be enough. In this case an image of the entire particular has been used as template and is

looked for in inspected image. The score of searching procedure is used as parameter to control; if the parameter is lower than a threshold fixed to 95%, the piece is rejected.
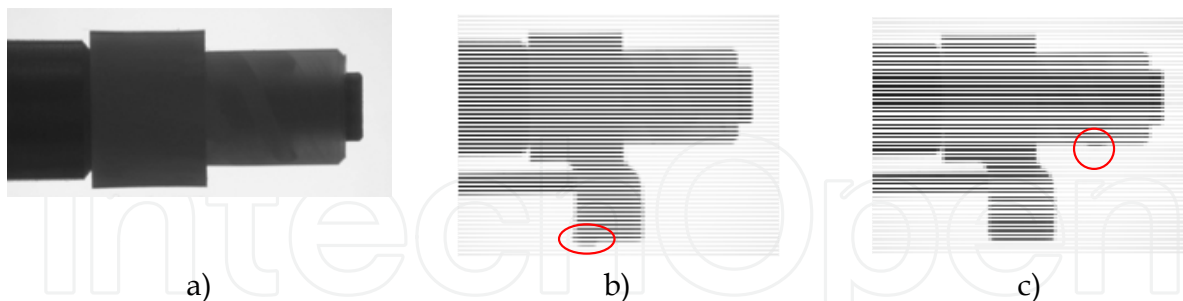

Fig. 16. Moulding injection process defects

For smaller defects, that give no significant changes in score of matching operation, it is necessary to adopt methods that analyze only limited parts of the image. For example, to find air bubble of fig. 15.c, the software search and identify the edge of the cylinder, then transforms points in a line with a linear regression and determines the residual of the operation as (Labview 8.2 User Manual, 2005):

$$r = \sqrt{\sum_i e_i^2} = \sqrt{\sum_i (y_i - y)^2} \qquad (4)$$

where, y_i represents the true point identified and y represent the point of the fitted line. If this parameter is higher than a fixed value, about 0.25 mm (corresponding to 15 pixel), it means that some discontinuity or irregularity is observed on the boundary surface (it doesn't matter if outwards or inwards) and part is rejected. The threshold value has been fixed analysing a sample of 100 good components and taking the bigger value founded.

The same method has been used for the air bubble on the ribbing, but in this case the edges identified and inspected are two, the same that can present the defects.

6. System performances

In this section, performances of the system, in terms of measurement precision and time saving, will be showed.

As example, the part of fig. 9.a has been used. In fig. 17, all the features to be determined are illustrated. There are four dimensional measurements, indicated as "D", a burr determination indicated as "Burr" and a shape defect identification, indicated by "screw end".

The description starts with dimensional measurement performance. Table 1 shows nominal dimension of requested features, and respective acceptable ranges.

To understand if the system is suitable to measure the required features and has a proper precision, repeatability and reproducibility, 100 images have been acquired from a component used as template, moving each time the part in the FOV to simulate a real measurement process, and resolution and standard deviation of results have been evaluated and compared with tolerance ranges.

About resolution, the system uses an image in which a pixel corresponds to 0,016 mm while the minimum tolerance range is 0,15 mm so, being their ratio approximately 10, the resolution can be considered suitable for the application.
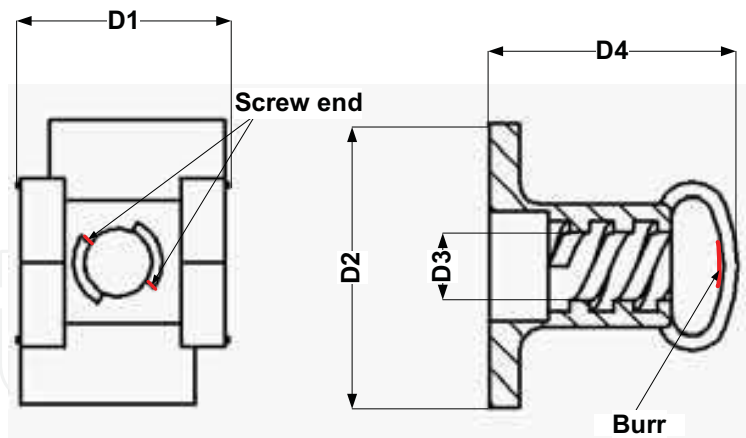
Fig. 17. The second component and the features to measure

	Nominal Dimension	Acceptable range
D1	14,00 mm	13,82÷14,18 mm
D2	19,50 mm	19,29÷19,71 mm
D3	4,80 mm	4,75÷4,90 mm
D4	17,00 mm	16,82÷17,18 mm
Burr		< 0,20 mm
Screw end		< 1,00 mm

Table 1. Feature to inspect

About repeatability, the results of 100 image measurements, on feature D1 as example, evidence a standard deviation of 0,0093 mm. Better results have been obtained with feature D2 and D4, respectively with standard deviation of 0,0055 mm and 0,0033 mm. The best result in repeatability is on D3 feature, with standard deviation of 0,0014 mm. These values include all possible disturbances, that is pixel noise and realignment errors, and can be considered as the accuracy of the instrument, because of the bias has been deleted choosing acquisition parameter settings that gives the same results as gauge measurements. About the process, results are reported in table 2.

With the exception of feature D3 (for which a comparison is not possible) it is evident that the average measures present minimum differences. This can be expected, because the image was calibrated on results of manual measurements. Standard deviation also are very similar.

Moreover, once the data has been stored, all statistical process evaluations are possible.

Assuming that the manufacture processes produce pieces whose dimensions or features are statistically scattered according to normal, or Gaussian, distributions, the process capacity can be automatically determined as (A. V. Feigenbaum, 1983):

$$Process\,Capacity = 6\sigma = \sqrt{\frac{\sum\left(u-\bar{u}\right)^2}{n-1}} \tag{5}$$

where: u = measurement of i^{nt} piece;

$\bar{u}$ = average value of measurements;

n = number of pieces evaluated.

The capacity ratio C_p and the performance index C_{pk} can be evaluated. For C_p evaluation the following equation has been used (J.M. Juran's, 1994):

$$C_p = \frac{USL - LSL}{6\sigma} \tag{6}$$

in which: ULS = Upper specification Limit;
LSL = Lower specification Limit;
6σ = Process capacity under statistical control.
The expression used for C_{pk} instead is (J.M. Juran's, 1994):

$$C_{pk} = \min(C_{up}; C_{low}) \tag{7}$$

where

$$C_{up} = \frac{USL - \bar{u}}{3\sigma} \tag{8}$$

$$C_{low} = \frac{\bar{u} - LSL}{3\sigma} \tag{9}$$

As example, table 2 reports process performances. In this case study the mould has 8 cavity, and each cavity has been measured 12 times. Totally, 96 pieces have been measured. Observing C_p results, it is noted that all measured features have an index superior to 1, so the process capability is adequate to meet established tolerance range. Moreover, the process has high repeatability, and feature D1, D2, and D4 have a C_p that ensure that no pieces can exceed tolerance range (in fact C_p is bigger than 1,63 that corresponds to 1 part per million). Only feature D3, because of a narrow tolerance range, have a C_p a bit lower alerting that a certain dispersion in production is occurring.

A further evaluation of results is possible by observing C_{pk}, in fact, C_{pk} values are lower, evidencing that the process is not centred with respect to the tolerance range. Worst situation is yet in feature D3, where C_{pk} is lower than 1; it means that a considerable percentage of pieces could exceed the tolerance limits. It's important to say, that presented data are about 8 different cavities of the mould; perhaps, dividing data per each cavity, only 1 cavity could present low C_p and C_{pk} indexes. Modifying dimensions of that cavity, indexes of the entire process could considerably increase.

		Average	Std. Dv.	C_p	C_{pk}
D1	Software	13,8960	0,0132	4,5455	1,9192
	Operator	13,9000	0,0135	4,4610	1,9827
D2	Software	19,4118	0,0153	4,5632	2,7814
	Operator	19,4110	0,0085	8,2440	4,7501
D3	Software	4,8570	0,0197	1,269	0,7276
	Operator				
D4	Software	17,0060	0,0290	2,0690	2,0000
	Operator	17,0050	0,0232	2,5896	2,5176

Table 2. Process performances

Also same consideration about reproducibility of the measurements are possible. To do this, two operators measured the same sample of pieces, once with the system and once with standard instruments. Table 3 reports these results.

		1 operator		2 operators	
		Software	Gauge	Software	Gauge
D1	Average	13,8960	13,9000	13,8970	13,8990
	Std. Dv.	0,0132	0,0135	0,0123	0,0124
D2	Average	19,4180	19,411	19,4130	19,4020
	Std. Dv.	0,0153	0,0085	0,0154	0,0134
D3	Average	4,8570		4,8540	
	Std. Dv.	0,0197		0,0194	
D4	Average	17,0060	17,0050	17,0050	16,9710
	Std. Dv.	0,0290	0,0230	0,0276	0,0397

Table 3. Reproducibility of measurements

It is possible to see that nothing is changed. Negligible differences are there between average values and standard deviation in both cases and consideration about process performances are also valid. On the contrary, measured values normally change passing from 1 to 2 operators with manual measurements, especially in feature D4 where is possible to notice a significant difference in average values (about 0,03 mm). Moreover, standard deviation increases in all cases, especially in D4, passing from 0,0230 to 0,0397. This is due to burr presence on the pieces (see fig. 11.a), as the software is able to avoid it from the measure, but this is not possible with standard instruments and the influence of the burr is different depending on the operator that is measuring. So it is possible to say that measurement process, doesn't change its precision passing from 1 to 2 operators, vice versa manually measuring, it loose precision and repeatability as higher is the number of operator. It means also, that Cp and Cpk decrease and the process could results out of control.

In fig. 18 are reported system performances about reproducibility for each feature.

Finally, once the data has been acquired, more and more quality control instruments can be automatically implemented, as example quality control chart (D. C. Montgomery, 1985).

About time saving, before explain the results, it is proper to describe the operations carried out both in manual and in optical controls.

In manual control, the operator have to execute the following steps in the order:
1.   Prepare sheet for registration;
2.   Control screw termination by a microscope;
3.   Measure burr entities by a contour projector;
4.   Measure feature D1, D2 and D4;
5.   Execute Functionality test (try to screw the coupled particular);
6.   Measure feature D3 with go-no-go gauge.

The order of the operation is important, because the entity of some feature can be changed during control. For example, go-no-go gauge control can damage the particular and functionality test can be compromised, as also screw termination can be damaged and incorrect consideration can be done by the operator.
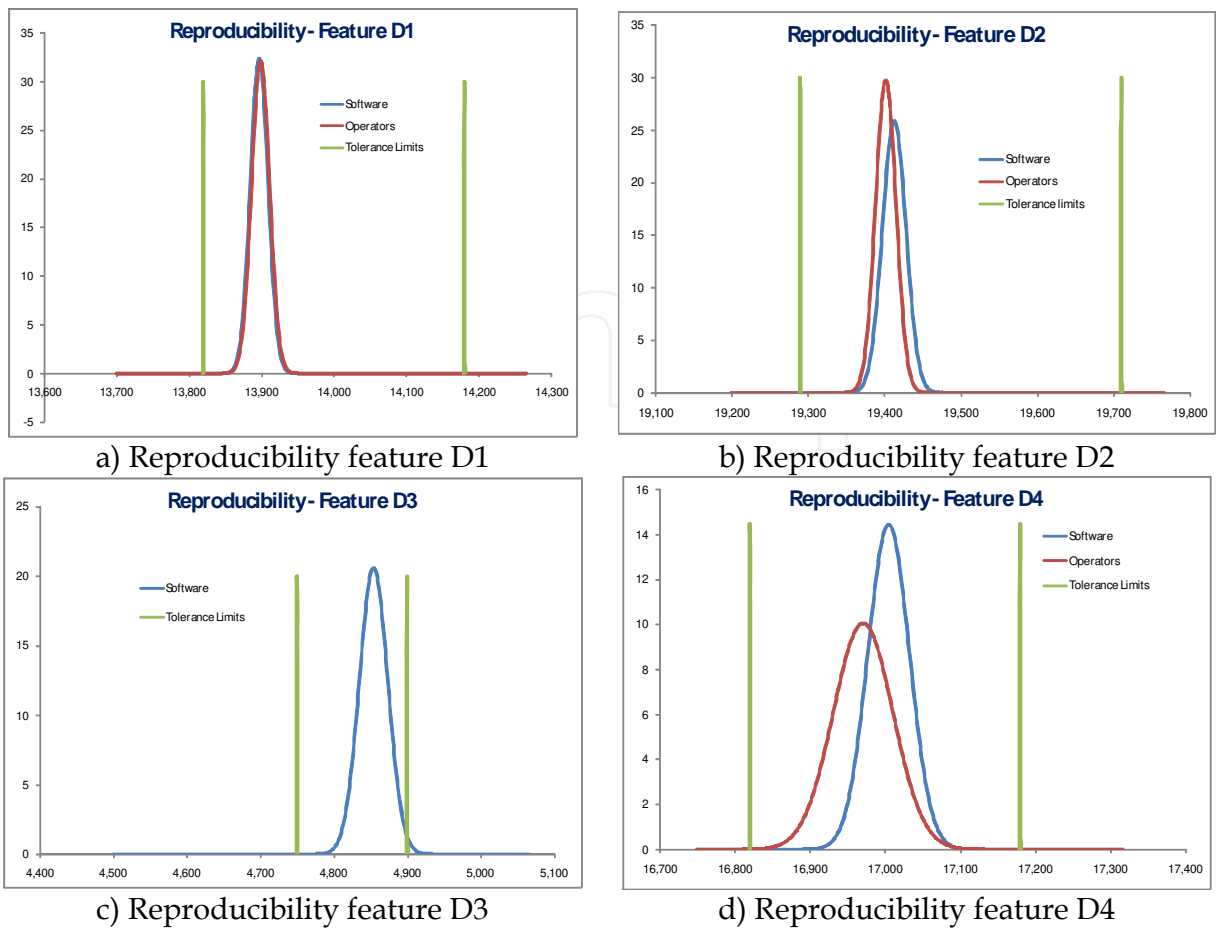
a) Reproducibility feature D1

b) Reproducibility feature D2

c) Reproducibility feature D3

d) Reproducibility feature D4

Fig. 18. Reproducibility of the measurements

a) Time needed for manual control

b) Time needed for automatic control

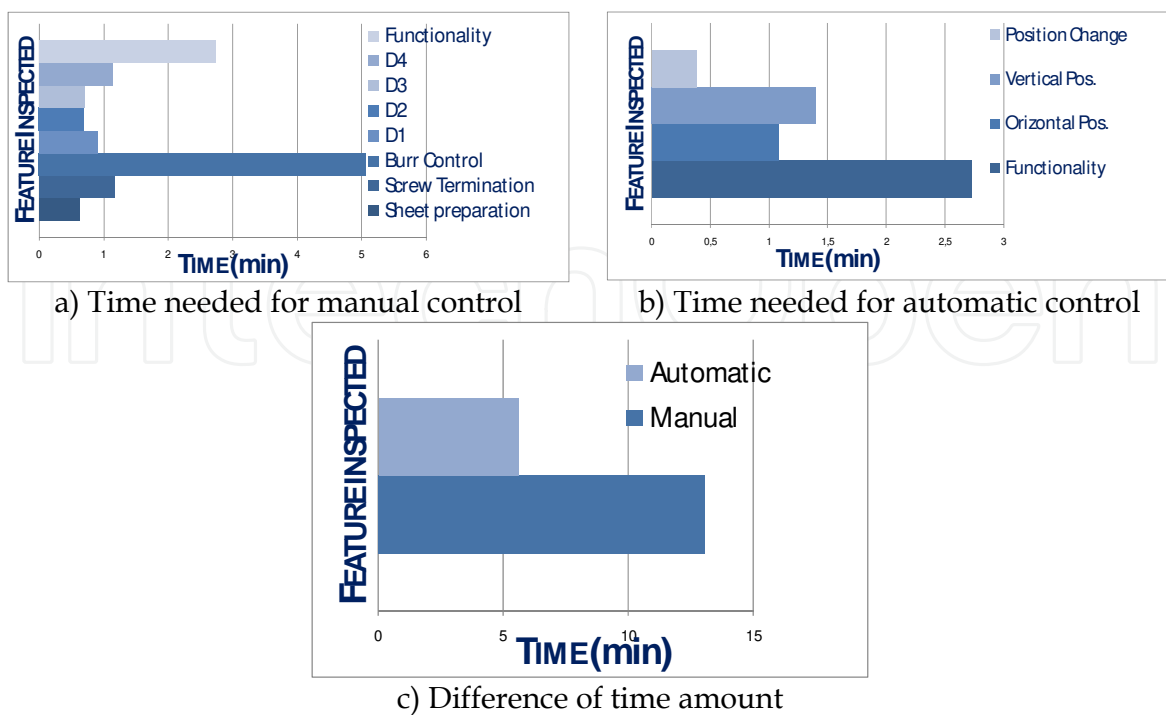c) Difference of time amount

Fig. 19.

Time needed for each operation is reported in fig 19.a; the values are referred to 8 pieces control.

Each bar represents the amount of time needed to measure the relative feature. It's clear from the picture, that the longest control is burr determination with over 5 minutes. Then, functionality test requires about 3 minutes and all the other feature requires about 1 minutes. The amount of time needed is reported in fig. 19.c (dark blue), and is over 13 minutes.

In automatic control instead, the procedure used is different: the particular is positioned first in a vertical position in the FOV of the system (figure 17 left) and the software determines feature D1, D2, D3 and screw termination. Then the particular is moved in an horizontal position (fig. 17 centre) and the software determines feature D4 and burr entity. The time for change particular position has also been considered. Finally, functionality tests have been executed as in the previous case.

Now, the longest control is functionality test, while horizontal and vertical position requires respectively 1 minute and 1 minute and a half. Change position requires about 40 seconds. The amount of time needed for the control is about 6 minutes (fig 19.c, light blue bar).

The big time reduction (near 54%) is due to different factors.

First of all, more than a feature can be measured at the same time, using the same instrument. So, as example, measure features D1, D2, D4 and screw termination (vertical position), that requires three different instruments in a time of about 3 minutes and a half, can be measured with only one instrument in only 1 minute.

Second, the reduction of time amount also depends on the net time reduction in single feature inspection. For instance, burr determination in manual process requires over than 5 minutes, while in automatic process requires only 1 minutes and a half (together with feature D4).

Finally, time for sheet preparation and registration has been deleted, because data are automatically stored and organized in a report that can be printed if necessary.

To close this section, some limits of the system will be listed.

First of all, only particulars (or features) with dimension smaller than the maximum FOV can be inspected. So larger components have to be controlled with a different system.

Second, precision of the system depends of FOV dimension. In fact, as bigger is FOV, as lower is precision of measurement because of the number of pixel of camera sensor is constant. Third, only feature that lies in a plane or with a depth lower than depth of focus can be inspected.

7. Aesthetic applications

Digital image processing can be used also for aesthetic control.
Possible application with the developed system are three:
1. Intensity colour determination;
2. Uniformity colour determination;
3. Detection of small black-dots.
All these application are based on histograms obtained by the image.
The histogram consists in counting the total number of pixel at each level of the greyscale. The graph of an histogram is a very quick way to distinguish if in the image there are regions with different grey-level value. Histograms are useful also to adjust the image and to optimize image acquisition conditions.

The histogram is the function *H* defined on the grayscale range *[0,…,k,…,255]* such that the number of pixels equal to the grey-level value *k* is (NI Vision Concept Manual, 2005):

$$H(k) = n_k \qquad (10)$$

where: k is the gray-level value,
   n_k is the number of pixels in an image with a gray-level value equal to k,
   n = Σn_k (from k=0 to 255) is the total number of pixels in an image.

The histogram plot reveals easily which gray level occurs frequently and which occurs rarely.

Two kind of histogram can be calculated: linear and cumulative histograms. In both cases the horizontal axis represents the gray-level value that ranges from 0 to 255.

For linear histogram, vertical axis represents the number of pixels n_k set to the value k. In this case, the density function is simply given by (10).

The probability density function is (Gonzalez & Woods, 1992):

$$P_{Linear}(k) = n_k / n \qquad (11)$$

where $P_{Linear}(k)$ is the probability that a pixel is equal to *k*.

For cumulative histogram instead, the distribution function is (NI Vision Concept Manual, 2005):

$$H_{Cumulative}(k) = \sum\nolimits_{i=0}^{k} n_i \qquad (12)$$

where $H_{Cumulative}(k)$ is the number of pixels that are less than or equal to *k*. The cumulated probability function is (NI Vision Concept Manual, 2005):

$$P_{Cumulative}(k) = \sum\nolimits_{i=0}^{k} \frac{n_i}{n} \qquad (13)$$

where $P_{Cumulative}(k)$ is the probability that a pixel is less than or equal to *k*. For the application illustrated below, only linear histograms will be used.

7.1 Colour intensity determination

First application has the aim to determine colour intensity of aesthetic goods. The problem is due to the production process, in fact for this kind of products, only a mould is used and different colours of the same particular are obtained mixing masterbatch colour to the virgin polymer and also recycled material (like sprue and cold runners). If the mixing process is not constant and regular, different percentage of colour can be mixed and the particular can be darker or lighter of the master. Figure 20.a show the PP cap here examined as example.

To determine the intensity of the colour the software acquires an image, from which extracts a portion; figure 20.b shows the acquired image and the extracted area in the yellow rectangle. On the extracted image, it calculates the histogram and the mean value of gray-level intensity of the pixels.

From figure 21 it is evident that the mean value of the histogram of the dark particular (grey-level=41,54) is lower than mean value of histogram of bright one (grey-level=64,21). So, it is possible to set a range of median value in which the extracted image have to be comprised. In this example, six ranges have been determined (figure 22 from a to f) to

separate different intensity colours. For each group the median grey-level intensity is reported below. Consider that six groups represent a resolution approximately three times bigger than human control (where only two groups are usually determined) and with much more objectivity.

|a) The particular examined|b) The area extracted|

Fig. 20. The particular examined

Finally, it must be noted that it is possible to deal with coloured parts by means of a monochromatic camera only if one is interested in measuring the colour intensity; obviously no considerations can be done on colour tonality. So the system is able to detect problems of incorrect mixing (as showed in next section) or insufficient/excessive masterbatch in the mix, but it cannot guarantee that the masterbatch used is correct.
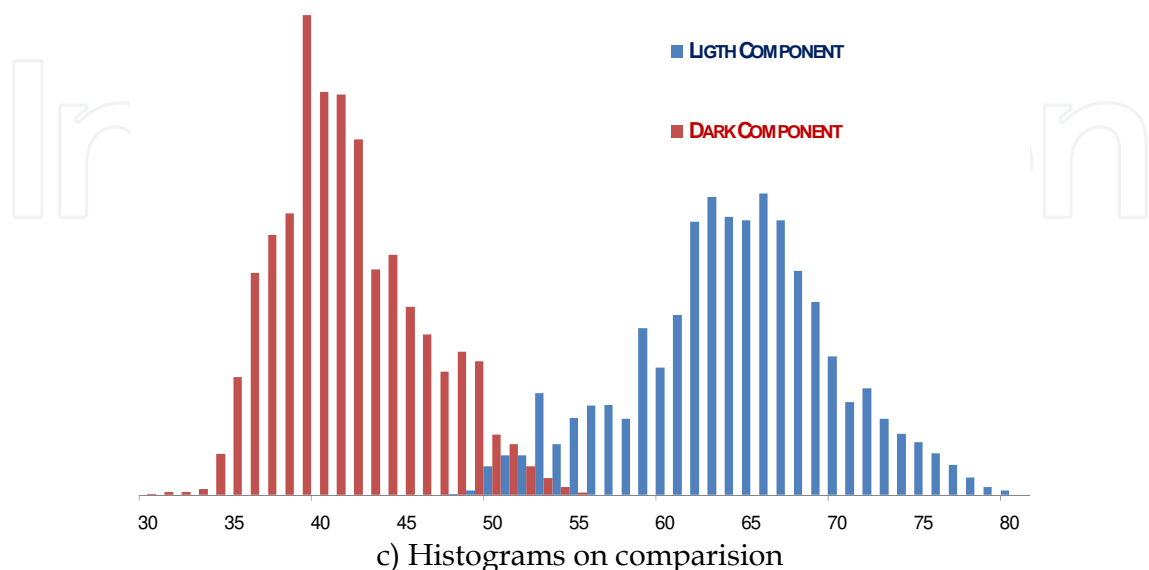

a) A light particular   b) A dark particular

c) Histograms on comparision

Fig. 21. Analysis of a light (a) and a dark (b) component by histogram (c)

a) 35 ÷ 45   b) 45 ÷ 50   c) 50 ÷ 55

d) 55 ÷ 60   e) 60 ÷ 65   f) 65 ÷ 70

Fig. 22. Six groups of different intensity colours

7.2 Colour uniformity determination

The second application developed regards the mixing problems between virgin polymer and masterbatch colour. In this case, components appears with non uniform colour as showed in figure 23. Figure 23.a shows a particular in which white material hasn't been correctly mixed, while the component of Figure 23.b was obtained with a correct mixing, with uniform rose. Figures 23.c and 23.d show the acquired images of the same particulars with the system. Extracting the same area from the images, as illustrated in fig. 20b, the histograms of figure 23e are obtained; it's evident that histogram of first particular has a standard deviation bigger than the second. So, it is possible to establish a tolerance range in which the variation can be accepted while outside the parts have to be discharged.
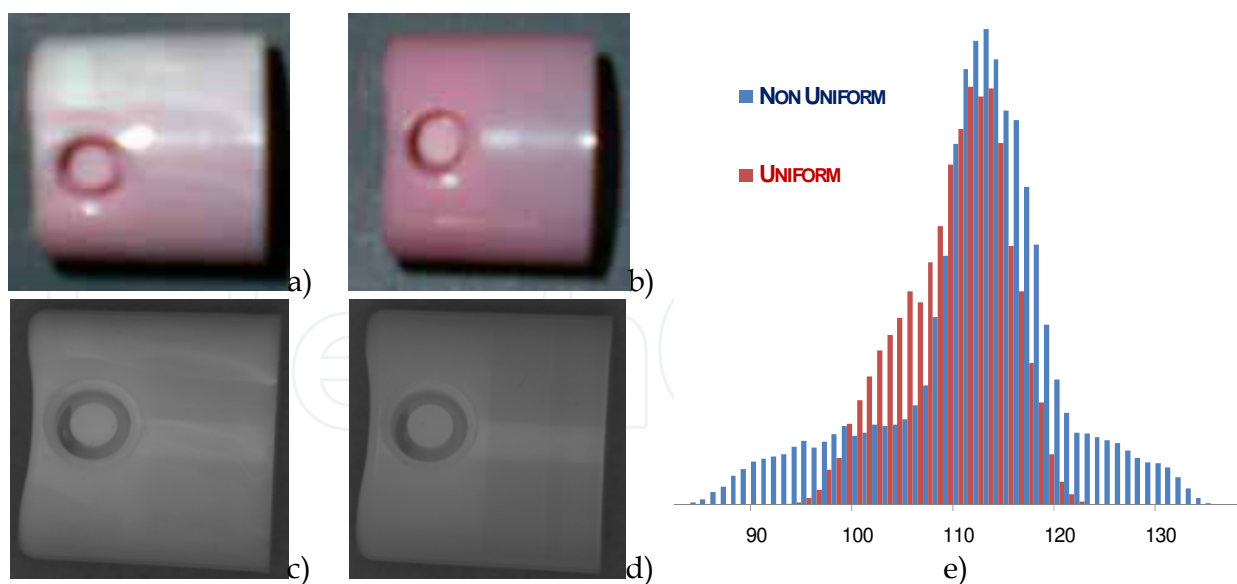

Fig. 23. Example of non uniform colour

7.3 Detection of small black dots

This problem is generally due to small impurities included in the material, which appear as small dots in the final product. Often, this kind of control is still demanded to visual inspection of expert operators, who look at the particulars from a distance of about 40 cm,

and if they can see the black dots the pieces are rejected. In this way, the control totally depends on the operator judgment and is totally arbitrary.

The optical system here presented uses an algorithm based on particle analysis: firstly it performs a binarization, finding all pixels with an intensity value lower than a fixed threshold; then, it considers all the particles (agglomerates of pixels) and counts the number of pixels each particle is made of. So, by knowledge of the pixel size in real dimensions, it is yet possible to establish maximum dimension of acceptable black dots, and the control will not depend from the operators estimation.

In fig. 24 a cap with black dots of different dimensions is reported. In this case the software looks for object with dimension bigger than 4 pixels. Dots with dimension bigger than the threshold value are highlighted in red circles, while black dots smaller than four pixels are highlighted in green circles. If only green circles are present, the piece can be accepted, while if red circles are present, the piece have to be rejected.
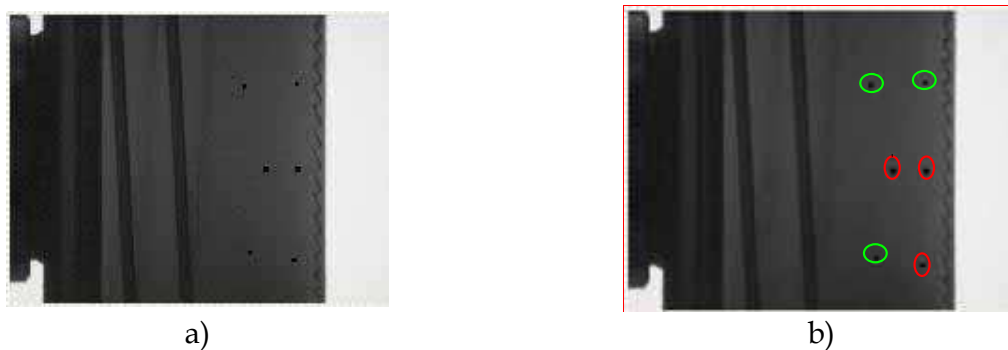

a)   b)

Fig. 24. An example of black dots on a particular

8. References

Feigenbaum A.V. (1986), *Total quality Control*, McGraw-Hill, 0-07-020353-9, Singapore.

Gonzales R. C.; R. E. Woods (1992), *Digital image processing*, Addison-Wesley, 0-201-50803-6, United States of America.

Juran J.M.; F.M.Gryna (1988), *Juran's quality control handbook fourth edition*, McGraw-Hill, 0-07-033176-6, United States of America.

Montgomery D. C. (1985), *Introduction to statistical quality control*, j. Wiley & sons, 0-471-80870-9, New York.

National Instruments (2005), *Labview user manual*

National Instruments (2005), *NI Vision concept manual*

Russ J.C. (1994); *The image processing handbook second edition*, CRC Press, 0-8493-2516-1, United States of America.

Applications and Experiences of Quality Control

Edited by Prof. Ognyan Ivanov

The rich palette of topics set out in this book provides a sufficiently broad overview of the developments in the field of quality control. By providing detailed information on various aspects of quality control, this book can serve as a basis for starting interdisciplinary cooperation, which has increasingly become an integral part of scientific and applied research.

How to reference

In order to correctly reference this scholarly work, feel free to copy and paste the following:

Marco Sasso, Massimo Natalini and Dario Amodio (2011). Digital Image Processing for Quality Control on Injection Molding Products, Applications and Experiences of Quality Control, Prof. Ognyan Ivanov (Ed.), ISBN: 978-953-307-236-4, InTech, Available from: http://www.intechopen.com/books/applications-and-experiences-of-quality-control/digital-image-processing-for-quality-control-on-injection-molding-products

INTECH
open science | open minds